

Using data and model to infer climate and environmental changes during the Little Ice Age in tropical West Africa

Anne-Marie Lézine¹, Maé Catrain¹, Julián Villamayor^{1,2} and Myriam Khodri¹.

1. Laboratoire d'Océanographie et du Climat. Expérimentation et Approche numérique/IPSL. Sorbonne Université-CNRS-IRD-MNHN. 4 Place Jussieu. 75005. Paris. France

2. Department of Atmospheric Chemistry and Climate, Institute of Physical Chemistry Rocasolano, CSIC, Madrid, Spain.

Abstract

Here we present hydrological and vegetation paleo-data extracted from 28 sites in West Africa from 5° S to 19° N and the past1000/PMIP4 IPSL-CM6A-LR climate model simulations covering the 850-1850 CE period to document the environmental and climatic changes that occurred during the Little Ice Age (LIA). The comparison between paleo-data and model simulations shows a clear contrast between the area spanning the Sahel and the Savannah in the North, characterized by widespread drought, and the equatorial sites in the South, where humid conditions prevailed. Particular attention was paid to the Sahel, whose climatic evolution was characterized by a progressive drying trend between 1250 and 1850CE. Three major features are highlighted: (1) the detection of two early warning signals around 1170 and 1240CE preceding the onset of the LIA drying trend; (2) a tipping point at 1800-1850CE characterized by a rainfall drop and an environmental degradation in the Sahel; and (3) a succession of drying events punctuating the LIA, the major of which was dated around 1600CE. The climatic long-term evolution of the Sahel is associated with a gradual southward displacement of the Inter-Tropical Convergence Zone induced by the radiative cooling impacts of major volcanic eruptions that have punctuated the last millennium.

1. Introduction

Precipitation in tropical West Africa is closely related to the West African Monsoon (WAM) system, created by the temperature land-sea contrast between the tropical Atlantic and the west of the African continent (Nicholson 2013) and is also influenced by the migration of the Inter Tropical Convergence Zone (ITCZ, Gagdil 2018). The WAM long-term variability during the 20th century has focused much attention due to the severe consequences in the Sahel semi-arid region, which experienced a long period of drought in the 1970-80s (Folland et al. 1986; Giannini et al. 2003). It is broadly accepted that these changes were mainly driven by the sea surface temperature (SST) variability (Folland et al. 1986; Mohino et al. 2011; Rodríguez-Fonseca et al. 2015), amplified by land surface processes (Giannini et al. 2003; Kucharski et al. 2013). However, only a few works document the WAM variability prior to the 20th century (Nicholson et al. 2012; Gallego et al. 2015; Villamayor et al. 2018) due to the little information covering the 19th century and beyond. The paleo-archives are rare, often incomplete, and suffer from often poorly constrained chronologies. Moreover, these archives are rarely direct records of climate parameters, but indirect ones, namely historical, biological, or sedimentological. They integrate not only changes in environmental parameters but also the vital effect of species, the vulnerability or the resilience of ecosystems and the cultural

¹ Corresponding author : anne-marie.lezine@locean.ipsl.fr

45 adaptations of populations. Here we use pollen and other environmental proxies as well as
 46 historical chronicles to document the last millennium with a special focus on the period from
 47 1250 to 1850 CE including the transition between the Medieval Climate Anomaly (MCA; 950-
 48 1250CE) and the Little Ice Age (LIA; 1450-1850CE) periods characterised by global
 49 temperatures respectively above and below average (Nash et al. 2016). The aim of this
 50 research is not to record the climate variability at interannual scale but to discuss the timing,
 51 distribution and magnitude of the major secular environmental changes which punctuated
 52 the LIA in northern tropical Africa with a focus on the regional biomes and hydrological
 53 systems responses times to rainfall anomalies.

54 2. Material and method

55 2.1 Paleo-data

56

57 This paper uses compilations of paleo-records from different sources with the highest
 58 available resolution (Table 1; Fig. 1). These data have the advantage of providing continuous
 59 records over the last millennium, but their temporal resolution is generally mostly
 60 (multi)decadal to centennial : pollen data are used for vegetation reconstructions (Elenga
 61 1992 ; Reynaud-Farrera et al. 1996; Ballouche 1998; Vincens et al. 1998; Salzmann et al. 2005;
 62 Ngomanda et al. 2007; Waller et al. 2007; Brncic et al. 2009; 2017; Lézine et al. 2011; 2013;
 63 2019; Lebamba et al. 2016; Tovar et al. 2019; Fofana et al. 2020; Catrain 2021), and
 64 micropaleontological, sedimentological and geochemical data to capture hydrological and
 65 climatic changes (Bertaux et al. 1998 ; Holmes et al. 1999 ; Street-Perrott et al. 2000 ; Schefuss
 66 et al. 2005 ; Wang et al., 2008 ; Shanahan et al. 2009 ; Mulitza et al. 2010 ; Nguetsop et al.
 67 2010 ; 2011 ; 2013 ; Carré et al. 2019 ; Lézine et al. 2019 ; Fofana et al. 2020 ; Catrain 2021).
 68 Compilations of historical chronicles (Nicholson 1978; 1980; 2013; Nicholson et al. 2012;
 69 Coquery-Vidrovitch 1997; Maley and Vernet 2013) and instrumental records (Gallego et al.
 70 2015) have also been examined, although the first are based on records of extreme events
 71 only (droughts, floods) and the second are limited in their temporal coverage. All these data
 72 are also scattered in a few limited areas of the Sahel (Senegal, Southern Mauritania, Niger
 73 River inner loop, Lake Chad basin) with possible redundancies.

74 The resulting data set is highly heterogeneous. Therefore, the data have been homogenized
 75 as follows: (1) only records covering the interval between 900 CE and present day with at least
 76 a 100-year temporal resolution have been taken into account, (2) in order to evaluate the
 77 relative amplitude of the environmental/climate change, we build a 6-point scale ranging from
 78 0, corresponding to the most arid environment (e.g., drying of lakes, salinization of water,
 79 increase of dust transport, bare soils) or the driest climate, up to 6, which refers to the most
 80 humid environment (e.g., high lake level, fresh water, dense forest) or the wettest climate.
 81 Decimal values were punctually added to identify minor changes in the paleoenvironment.
 82 This approach, based on our own expertise, provides a *qualitative* description of regional
 83 environmental and climatic conditions. It emphasises the major stages of environmental
 84 change while eliminating minor noisy variations (see supplementary Figure).

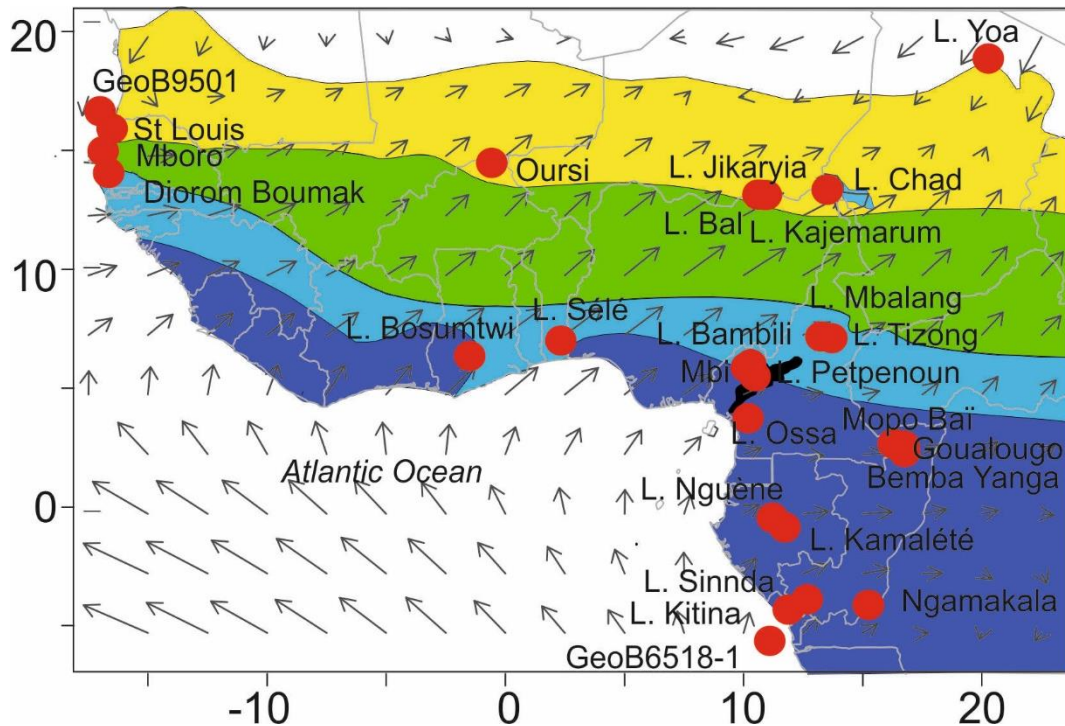
85

Site name	proxy	latitude	longitude	reference	Sector/vegetation zones
Lake Yoa	Pollen/sediment	19.057621	20.500690	Lézine et al. 2011	Sahara (Desert)

GeoB9501	Dust fraction	16.83333	-16.73333	Mulitza et al. 2010	Sahel
St Louis	Pollen/Diatom	16.03508	-16.48382	Fofana et al. 2020	Sahel (grasslands and wooded grasslands)
Mboro (Baobab)	Pollen/Diatom	15.149132	-16.909275	Lézine et al. 2019	Sahel (grasslands and wooded grasslands)
Oursi	Pollen	14.65283	-0.486	Ballouche 1998	Sahel (grasslands and wooded grasslands)
Dioron Boumak	Geochemistry	13.835809	-16.498372	Carré et al, 2019	Sahel/Savannah boundary
Lake Jikaryia	Sediment/Mineral-magnetic	13.3136667	11.077	Waller et al. 2007; Wang et al. 2008	Sahel (grasslands and wooded grasslands)
Lake Bal	Ostracods/Chemistry	13.304	10.943	Holmes et al. 1999	Sahel (grasslands and wooded grasslands)
Lake Kajemaru m	Dust fraction/Geochemistry	13.303	11.024	Street-Perrott et al. 2000	Sahel (grasslands and wooded grasslands)
Lake Chad	Historical	13.053472	14.463469	Maley and Vernet 2013	Sahel (grasslands and wooded grasslands)
Lake Mbalang	Pollen/Diatoms	7.316	13.733	Vincens et al. 2000; Nguetsop et al. 2011	Savannah
Lake Tizong	Pollen/Diatoms	7.25	13.583	Nguetsop et al. 2013; Lebamba et al. 2016	Savannah
Lake Sélé	Pollen	7.15	2.433	Salzmann et al. 2005	Savannah
Lake Bosumtwi	Geochemistry	6.5	-1.416	Shanahan et al. 2009	Central Africa (lowlands) (Equatorial forests)
Mbi	Pollen	6.089273	10.348549	Lézine et al., in press	Central Africa (highlands) (Afromontane forests)

Lake Bambili	Pollen/ Geochemistry	5.936	10.242	Lézine et al. 2013	Central Africa (highlands) (Afromontane forests)
Lake Petpenoun	Pollen	5.64147	10.64531	Catrain 2021	Savannah
Lake Ossa	Pollen/Diatoms	3.800	10.75	Reynaud Farrera et al. 1996; Nguetsop et al. 2010	Central Africa (lowlands) (Equatorial forests)
Mopo Bai	Pollen/Geochemistry	2.240	16.261388	Brncic et al. 2009	Central Africa (lowlands) (Equatorial forests)
Bemba Yanga	Pollen	2.18726	16.52513	Tovar et al. 2019	Central Africa (lowlands) (Equatorial forests)
Goualougo	Pollen	2.0875	16.54722	Brncic et al. 2017	Central Africa (lowlands) (Equatorial forests)
Lake Nguène	Pollen	-0.2	10.466	Ngomanda et al. 2007	Central Africa (lowlands) (Equatorial forests)
Lake Kamalété	Pollen	-0.7166	11.7666	Ngomanda et al. 2007	Central Africa (lowlands) (Equatorial forests)
Lake Sinnda	Pollen/Sediment	-3.836111	12.8	Bertaux et al. 1996 ; Vincens et al. 1998	Central Africa (lowlands) (Equatorial forests)
Ngamakala	Pollen	-4.075	15.38333	Elenga 1992	Central Africa (lowlands) (Equatorial forests)
Lake Kitina	Pollen/Sediment	-4.27	12	Bertaux et al. 1996 ; Elenga et al. 1996	Central Africa (lowlands) (Equatorial forests)
GeoB6518-1	Alkenone / Geochemistry	-5.588333	11.221667	Schefuss et al. 2005	Central Africa

87 Table 1: Geographical positions, type and references of paleo-records used in this study (see
 88 Fig. 1).
 89

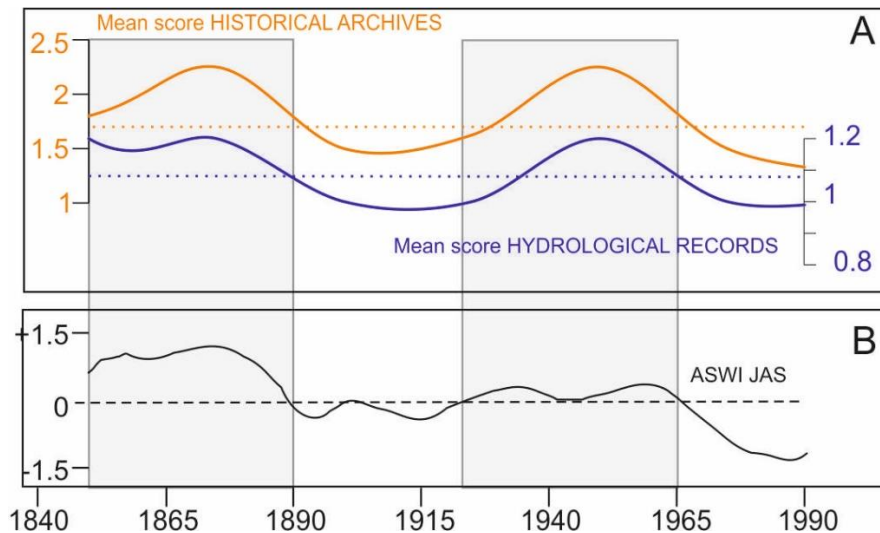


90
 91 **Figure 1:** Map showing the location of paleorecords available in tropical West Africa
 92 documenting the last millennium (Table 1). Grey arrows indicate the strength and direction
 93 of the main 925 hPa monsoonal winds during boreal summer, i.e., the WAM rainy season
 94 (NCEP-DOE AMIP-II Reanalysis (Kanamitsu et al., 2002)). In color, vegetation units from White
 95 (1983): dark blue: Guineo-Congolian rainforest; light blue: Sudano-Guinean woodland and
 96 wooded grassland (here referred to as Savannah (vegetation) zone); green: Sudanian
 97 woodland and wooded grassland; yellow: Sahelian grassland and wooded grassland. black:
 98 Afromontane forest.

99

100 In order to verify whether the methodology employed provides reliable indications of
 101 environmental change for the period prior to the instrumental records scores of the WAM
 102 rainy season (July to September), multidecadal hydrological changes from natural archives and
 103 historical data (Table 1) in the Sahel are compared to the African Southwesterly Index (ASWI)
 104 developed by Gallego et al. (2015) over 1840-1990 CE. The ASWI is based on JAS wind direction
 105 data (i.e the persistence of the low-level southwesterly winds) from historical measurements
 106 available since 1839 in a region over the Atlantic, close to West Africa (29°W–17°W, 7°N–
 107 13°N). The ASWI is strongly correlated with the observed Sahel precipitation since 1900 and
 108 is, therefore, presented as a good indicator of its variability. It was validated against
 109 instrumental observations as a good measure of WAM intensity during the rainy season over
 110 the instrumental period (Gallego et al. 2015). Positive values of the ASWI indicate periods
 111 when the monsoon is well established over the Sahel, and thus define periods of heavy rainfall
 112 in the region, which is consistent with observational data (Descroix et al. 2015). As previously
 113 shown by Villamayor et al. (2018), there are strong similarities between the historical rainfall
 114 records in the Sahel and ASWI. However, Figure 2 shows that historical records (yellow curve,
 115 Figure 2A) give a slightly different magnitude of dry and wet anomalies that reflects the
 116 sensitivity of populations to periods of drought or flooding. Our assessment of hydrological

117 conditions based on natural archives (blue curve, Figure 2A) reflects historical records
 118 variations but with a somewhat weaker magnitude. This is probably due to the much lower
 119 temporal resolution of the available data (25-50 yrs on average). It is also worth noting that
 120 the lake data corresponds to a precipitation/evaporation balance and not the precipitation
 121 amounts at a given site. Nevertheless, the curves are remarkably similar and point to wet
 122 periods centred ca 1875 and 1950 CE.
 123



124
 125

126 **Figure 2:** Observed and reconstructed rainfall anomalies over the Sahel during the 1840-1990
 127 CE period. (A) the mean scores from historical (yellow curve) and natural archives (blue curve)
 128 for the Sahel (Nicholson, 1978; 1980; Nicholson et al. 2012; 2013; Coquery-Vidrovitch, 1997;
 129 Holmes et al., 1999; Street-Perrott et al. 2000; Waller et al. 2007; Wang et al. 2008; Mulitza et
 130 al. 2010; Maley and Vernet, 2013; Lézine et al. 2019). The dotted yellow and blue lines
 131 correspond respectively to the historical and paleohydrological archives mean scores during
 132 the period 1850-1990CE. They allow identifying anomalously wet and dry periods. (B) The
 133 African Southwesterly Index (ASWI) developed by Gallego et al. (2015) as a measure of rainfall
 134 anomalies in Sahel during the WAM rainy season (July to September).
 135

136

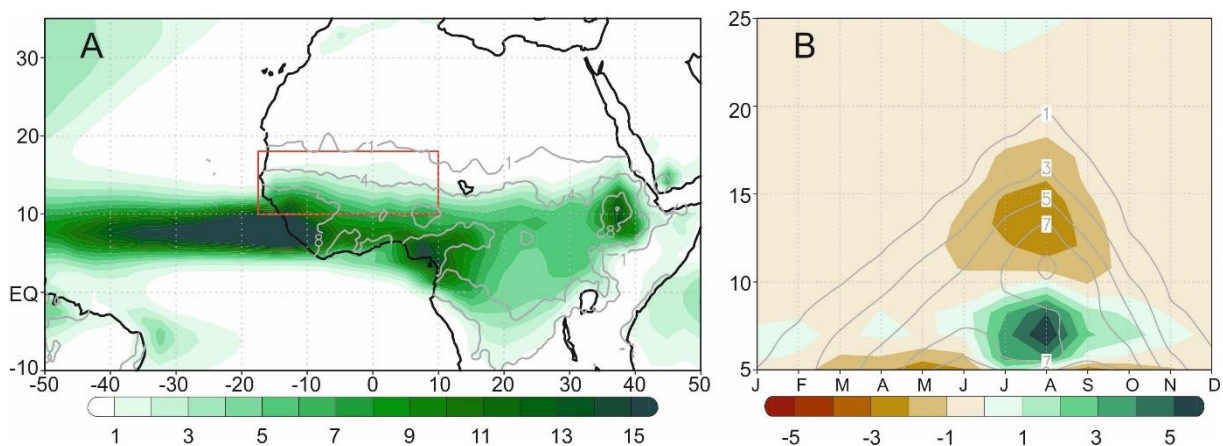
136 2.2 Model experiments

137 In this study we compare reconstructed environmental changes in Western Africa to those
 138 simulated in the past1000 model experiment covering the 850-1850 CE climate performed as
 139 part of 4th phase of the Paleoclimate Modelling Intercomparison Project (PMIP4; Jungclaus et
 140 al. 2017; Kageyama et al. 2017) by the IPSL-CM6A-LR model version developed for the Coupled
 141 Model Intercomparison Project phase 6 (CMIP6) at Institut Pierre-Simon Laplace (Boucher et
 142 al. 2020; Lurton et al. 2020). The IPSL-CM6A-LR model couples the atmospheric component
 143 LMDZ (Hourdin et al. 2020) to the land surface model ORCHIDEE (d'Orgeval et al., 2008) and
 144 to the ocean model NEMO, which includes other models to represent sea-ice interactions
 145 (Rousset et al., 2015) and biogeochemistry processes (Aumont et al. 2015). The atmospheric
 146 and land-surface grid have a resolution of 2.5° in longitude and 1.3° in latitude with 79 vertical
 147 layers. The oceanic component has 75 vertical levels with a mean spatial horizontal resolution
 148 of about 1° and a refinement of 1/3° near the equator. This model reproduces fairly well the
 149 ENSO (McPhaden et al. 2006) seasonality despite the sea surface temperature anomalies
 150 extending too westward in the central Pacific during El Niño events. The spatial pattern of the

151 Atlantic Multidecadal Variability (AMV, Deser et al. 2010) teleconnection in the Pacific is
 152 consistent with observations but the tropical Atlantic variability is relatively weaker. Unlike
 153 most current state-of-the-art CMIP6 models, the IPSL-CM6A-LR model simulates a
 154 predominant secular variability in the Atlantic with AMV peaks separated by about 200 years
 155 (Boucher et al., 2020).

156 The past1000 IPSL-CM6A-LR model experiment is designed to simulate the climate response
 157 to natural forcings recommended by PMIP4 (Jungclaus et al. 2017) and covering the pre-
 158 industrial millennium (850-1849CE), namely the time varying astronomical parameters, the
 159 trace gases (Meinshausen et al. 2017; Matthes et al. 2017), the eVolv2k volcanic forcing
 160 (Toohey and Sigl 2017), the SATIRE-M 14C solar activity with an adaptation of the spectral
 161 irradiance to the CMIP6 *historical* forcing and the land use forcing (Lawrence et al. 2016).
 162 Three past1000 IPSL-CM6A-LR model simulations have been performed and branched off from
 163 various initial conditions in a 600 years long spinup run with fixed external radiative forcing to
 164 the year 850 CE. This spinup run, itself branched off from the IPSL-CM6A-LR pre-industrial
 165 control (piControl) run with constant external radiative forcing, has been performed to avoid
 166 any spurious drift in the past 1000 experiments that could be related to the adjustment of the
 167 slow components of the climate system (such as the ocean), to the different radiative balance
 168 at the beginning of the last millennium as compared to the pre-industrial levels.

169
 170



171
 172

173 **Figure 3:** Climatological bias of simulated monthly precipitation. A) JAS mean averaged across
 174 (colors) the 2000-year piControl run and (contours) the 1891-2019 period in GPCPv2020
 175 observational database. B) (colors) Meridional seasonal cycle of the 10° W – 10°E mean model
 176 bias (simulation minus observations) compared to (contours) the GPCPv2020 climatology. All
 177 units are mm/day. Red box in (A) indicates the Sahel region (17.5°W-10°E; 10°-18°N).

178

179 The IPSL-CM6A-LR model reproduces the observed climatological distribution of maximum
 180 rainfall across West Africa during the WAM rainy season (Fig. 3A). The timing of the simulated
 181 WAM seasonal cycle is also in good agreement with observations, with a well-defined onset
 182 of the rainy season in July and then a demise after September (Fig. 3B). However, the
 183 northward shift of maximum rainfall over the Sahel during the rainy season is underestimated
 184 by the model by about 4° (the model's maximum in August is ~7°N and the observed one at
 185 11°N). As a result the climatological rain belt over West Africa is slightly more constrained to
 186 tropical regions compared to observations and dryer Sahel on average. However, the well-

187 characterized WAM seasonal timing suggests that there are no remarkable biases affecting
188 the simulated precipitation variability.

189 Then, to characterize the simulated Sahel rainfall multidecadal variability over the past
190 millennium and contrast to the reconstructed environmental series, an index is calculated as
191 the 10-year low-pass-filtered Sahel precipitation anomalies in the rainy season from past1000
192 simulations. Seasonal precipitation anomalies from July to September (JAS), relatives to the
193 piControl climatology, are area-weighted and averaged across the Sahel region (red box in Fig.
194 3A), then filtered with a 10-year centered moving mean with truncated endpoints (i.e., only
195 averaging existing elements within the 10-year window). An ensemble-mean index is also
196 performed to highlight the forced component of the Sahel multidecadal variability in response
197 to natural forcings that are common to the three past1000 members, such as the effect of
198 large volcanic eruptions, in contrast to the internal variability.

199

200 **3. Results**

201 **3.1 The hydrological records**

202

203 The hydrological records provide a contrasting picture from one region to another: the Sahel,
204 the Sudano-Guinean Savannah zone and the tropical forests. They also reveal some local
205 exceptions. As already noted (e.g., Vincens et al. 1999), the local hydrogeological context may
206 strongly affect the individual response of lakes and wetlands to rainfall variations and partly
207 explains this apparent heterogeneity.

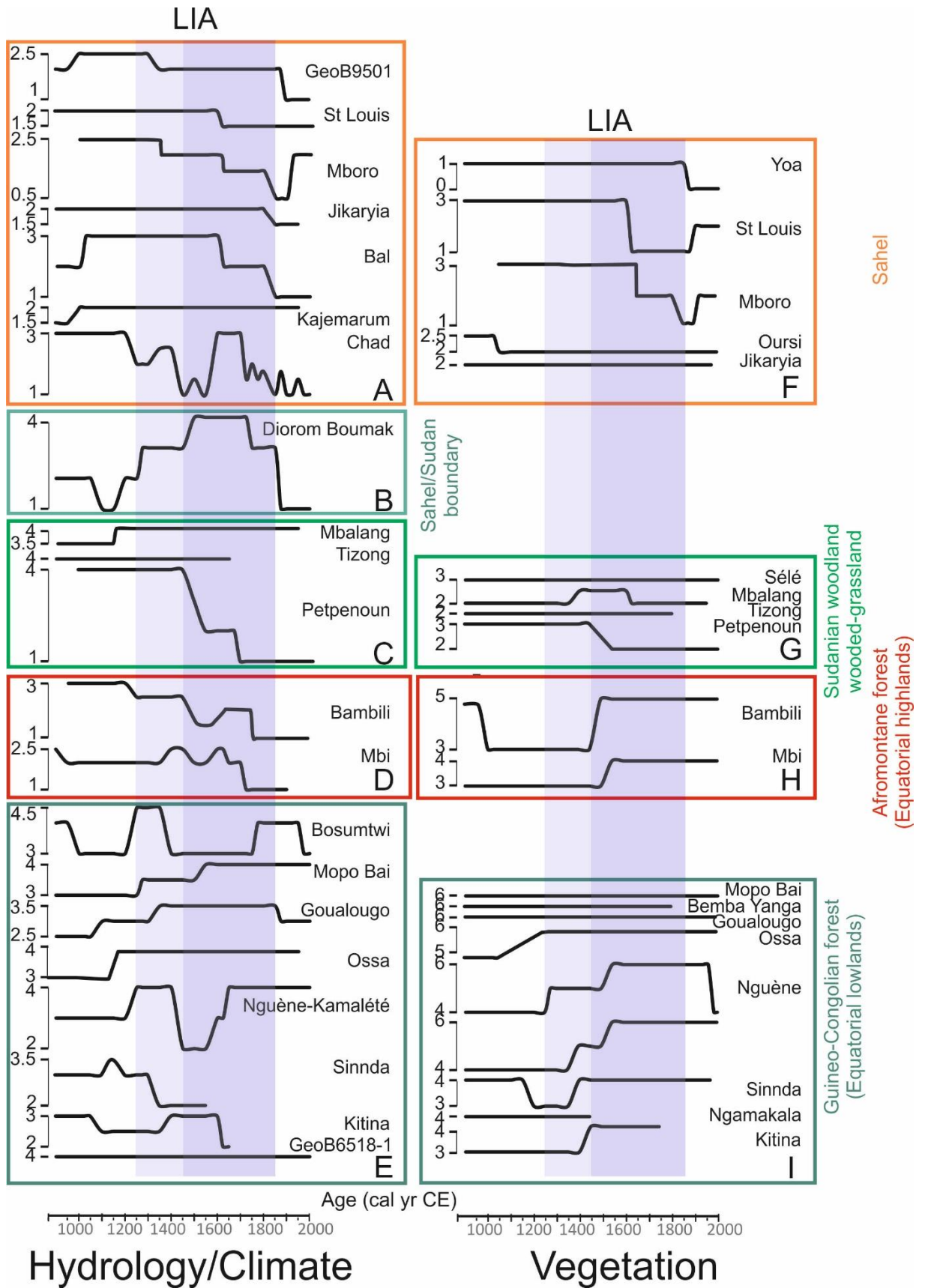
208 The main characteristics of the hydrological evolution in the Sahel, in the Savannah zone and
209 in low- and high-altitude equatorial forests can be summarized as follows (Fig. 4):

210 • Data from the central and western Sahel (Fig. 4A) point to a relatively dry period at the
211 end of the first millennium (900CE) at Bal, Kajemarum and in the Senegal River
212 watershed (GeoB9501). A wet period followed, already present at Mboro near the
213 littoral, which lasted up to 1350CE. Except at Kajemarum and Jikarya, where
214 hydrological conditions remained relatively stable, a gradual trend toward increased
215 aridity is recorded in two steps dated ca. 1625CE and 1800CE, respectively. Then,
216 during the last two centuries, only minor fluctuations occurred in a general context of
217 widespread aridity.

218 In the lake Chad area, Maley and Vernet (2013) depict a rather different and complex
219 history probably due to the variety of the archives they used (both historical and
220 natural) and also to the complexity of the hydrology of this immense water body
221 (Pham-Duc et al. 2020) fed by underground waters and by rivers of distant
222 geographical origin. The authors identify two major periods of flooding in the lake
223 Chad area: from the onset of the millennium to ca. 1200CE, then between 1600 and
224 1700CE, with a series of dry periods in between then from 1700CE onwards.

225 • Only three sites document the hydrological evolution of the Savannah zone south of
226 the Sahel (Fig. 4C). These sites are located in the centre of the savannah zone (White
227 1985): two crater lakes on the Adamawa plateaus (Mbalang and Tizong) and the other
228 at the mouth of the tributary of Lake Petpenoun in the Grassfields region of Cameroon.
229 The Adamawa lakes do not show any significant hydrological changes throughout the
230 last millennium. In contrast Petpenoun records a clear evolution towards aridity which
231 started ca. 1425CE and culminated ca. 1650CE up to the present day.

- 232
- 233
- 234
- 235
- 236
- 237
- 238
- 239
- 240
- 241
- 242
- 243
- 244
- 245
- 246
- 247
- 248
- 249
- 250
- 251
- 252
- 253
- Diorom Boumak (Fig. 4B) is situated at the southern boundary of the Sahel, in the littoral mangrove of the Saloum estuary. In contrast to the other sites from the Sahel and savannah zone this site records a remarkable wet period between 1500CE and 1800CE. As elsewhere however, aridification started ca. 1800CE.
 - The equatorial lowlands is characterized by contrasting hydrological situations reflecting the diversity of local hydrogeological settings (Fig. 4E). Low lake levels are recorded at Bosumtwi, Mopo Bai, Goualougo, Nguène-Kamalété and Ossa during a period centred around 1100CE in contrast to Sinnda and Kitina where moist conditions occurred. Moisture increased as soon as 1350CE at Goualougo and continued up to 1400CE at Mopo Bai and Kitina. Then, there is a clear opposition between Sinnda, Nguène-Kamalété and Bosumtwi where low lake levels occurred during a dry phase between ca 1350 and 1700CE and Mopo Bai, Goualougo, Ossa and Kitina, which are characterized by wetter conditions. In any case, the marine record at the mouth of the Congo River (GeoB6518-1) suggests that all these hydrological variations in the equatorial lowlands remained of relatively low amplitude.
 - In the Cameroon highlands (Fig. 4D), hydrological conditions steadily declined as shown at lake Bambili, starting from ca. 1250 and culminating ca. 1675CE. This gradual trend is interrupted ca. 1500CE by a more pronounced phase of lake level lowering. The Mbi swamp displays a rather different pattern: here, the water level was relatively low throughout the whole last millennium except to two discrete wetter phases ca. 1450 and 1650CE.



254
255
256
257
258

Figure 4: Mean scores of hydrological and vegetation changes along a North-South transect from the northern limit of the Sahel (Yoa) to the Congo basin (GeoB6518-1). Data are grouped within the phytogeographical entities defined by White (1983) in tropical Africa: Sahelian

259 grassland and wooded grassland, Sudano-Guinean savannah, highland Afromontane forest,
 260 lowland Guineo-Congolian forest. The environmental index (bold black line) shows the
 261 evolution of vegetation from bare soil (0) to dense forest (6). The intermediate values are 1:
 262 steppe/grassland; 2 : wooded grassland; 3: woodland/gallery forest; 4: degraded/secondary
 263 forest; 5: montane forest (panel F to I). For hydrology and climate, the index shows the
 264 evolution from dry (1) to wet (4) with intermediate values showing the gradation between
 265 these two extremes (panel A to E). The shaded vertical bands indicate the transition period
 266 between the medieval climate anomaly and the Little Ice Age (1250-1450CE light shading) and
 267 the LIA (1450-1850CE dark shading).

268

269 **3.2 Pollen data**

270

- 271 • In the open landscapes of the Sahara, Sahel and Savannah zones, vegetation changes
 272 were of minor amplitude except at sites where gallery forests were previously well
 273 developed. It is in the westernmost part of the Sahel that the most profound changes
 274 in vegetation cover are recorded : In the Niaye area (Mboro) and in the Senegal river
 275 delta (St Louis), the degradation of the landscape originated ca. 1300CE and
 276 accelerated ca. 1600CE to a maximum reached ca. 1850CE (Fig. 4F). A discrete
 277 vegetation recovery is then recorded in the 19th century. In contrast, sites from the
 278 central Sahel (Oursi and Jikarya) remained relatively stable throughout the last
 279 millennium in spite of a slight degradation recorded at Oursi ca. 1050CE. North of the
 280 Sahel (Yoa), the aridification of the desert landscape accelerated from the 19th century
 281 onward. South of the Sahel, in the Savannah zone, lakes Tizong and Sélé do not record
 282 any marked environmental change contrary to Petpenoun where a slight degradation
 283 is recorded ca. 1425CE (Fig. 4G). At Mbalang, a discrete phase of vegetation recovery
 284 occurred between ca 1400-1600CE.
- 285 • The forest cover remained roughly unchanged in the central forest massif (Mopo Baï,
 286 Bamba Yanga, Goulalougo, Fig. 4I). In the western regions by contrast, (Ngamakala,
 287 Kitina, Lac Ossa, Nguène and Kamalété the forest gradually developed since 1250-
 288 1350CE in spite of the discrete hydrological fluctuations. In the Cameroon highlands
 289 (Fig. 4H), the forest development occurred later, ca 1550-1500CE, after a phase of
 290 forest clearance from 1000 to 1450CE.

291

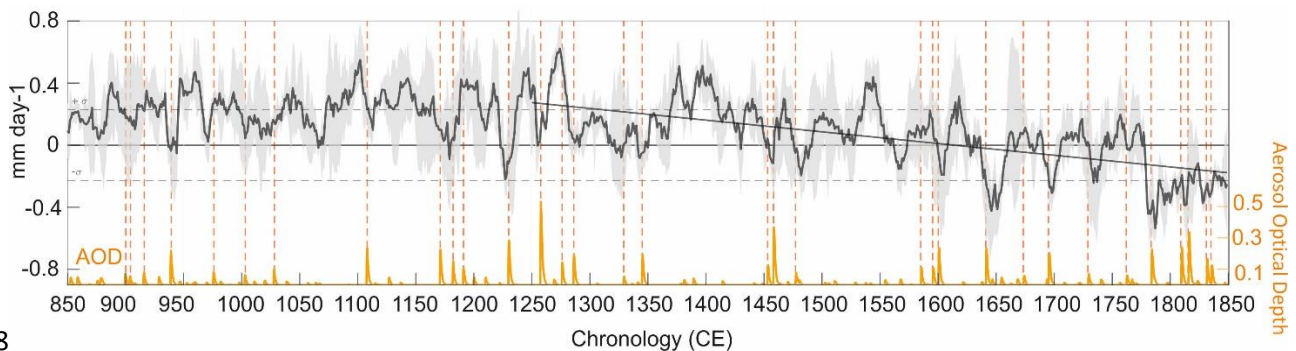
292 **3.3 Model results**

293

294 The index of the ensemble-mean Sahel JAS precipitation simulated over the past millennium
 295 reveals a change from a relatively wet mean state in the MCA (950-1249 CE) to a drier one in
 296 the LIA (1450-1849) (Fig. 5), suggesting a shift of the average WAM rainfall regime. Such
 297 continuous decline presents a linear rate of the seasonal Sahel rainfall of -0.7 mm per decade
 298 over 1250-1849CE, resulting in a 7% loss of the mean precipitation in the LIA relative to MCA
 299 (Fig. 5). Regarding decadal variations, the ensemble-mean index of past1000 Sahel
 300 precipitation almost doubles its variability in the LIA with respect to the MCA (the variance in
 301 859-1249CE is 51% higher than in 1450-1849CE), which suggests a more unstable rainfall
 302 regime, apart from drier on average, by the late past millennium in response to natural
 303 external forcings. Such a simulated long-term drying trend and increased LIA Sahel
 304 precipitation decadal variability is related to the volcanic forcing influence on SSTs, which
 305 integrates the induced radiative cooling (Fang et al. 2021). The more frequent large volcanic

306 eruptions during the LIA, as compared to the MCA, is integrated by the ocean long memory,
 307 leading to a gradual SST decrease that is more pronounced in the Northern Hemisphere than
 308 the Southern Hemisphere. The relative North Atlantic SST cooling trend along 850-1849CE,
 309 gradually promotes a southward shift of the Inter-Tropical Convergence Zone (ITCZ) and a
 310 weakening of monsoon moisture inflow to Western Africa. The long term WAM weakening is
 311 further amplified in the few years following any new large volcanic event, which occurrences
 312 are indicated by the vertical dotted lines on Figure 5. As a consequence, more frequent
 313 negative rainfall anomalies lasting at least 5 consecutive years are also evident during the LIA
 314 as compared to the MCA, with significant drying that can persist up to 60 years around clusters
 315 of eruptions such as those of the 19th century.

316
 317



318
 319

320 **Figure 5:** Multidecadal Sahel rainfall variability in IPSL-CM6A-LR past1000 simulations. Black
 321 line: 10-years low pass filtered index of Sahel JAS precipitation anomalies averaged in boxed
 322 area in Figure 3 (i.e., 10°-18°N and 17.5°W-10°E). The black line corresponds to the ensemble
 323 mean, the grey shading to the ensemble spread and diagonal line to the 1250-1849 CE linear
 324 fit. Dashed horizontal lines show the +/- standard deviation of the equivalent piControl index.
 325 The volcanic forcing used in the IPSL-CM6A-LR model experiments is shown by the orange
 326 curve as the globally averaged Aerosol Optical Depth (AOD). Red vertical dotted lines indicate
 327 the occurrence of strong volcanic eruptions about the size or larger than the Pinatubo eruption
 328 (June 1991) defined when the tropical (20°S-20°N) or northern extratropical (50°N-90°N)
 329 mean AOD is larger than 0.1.

330

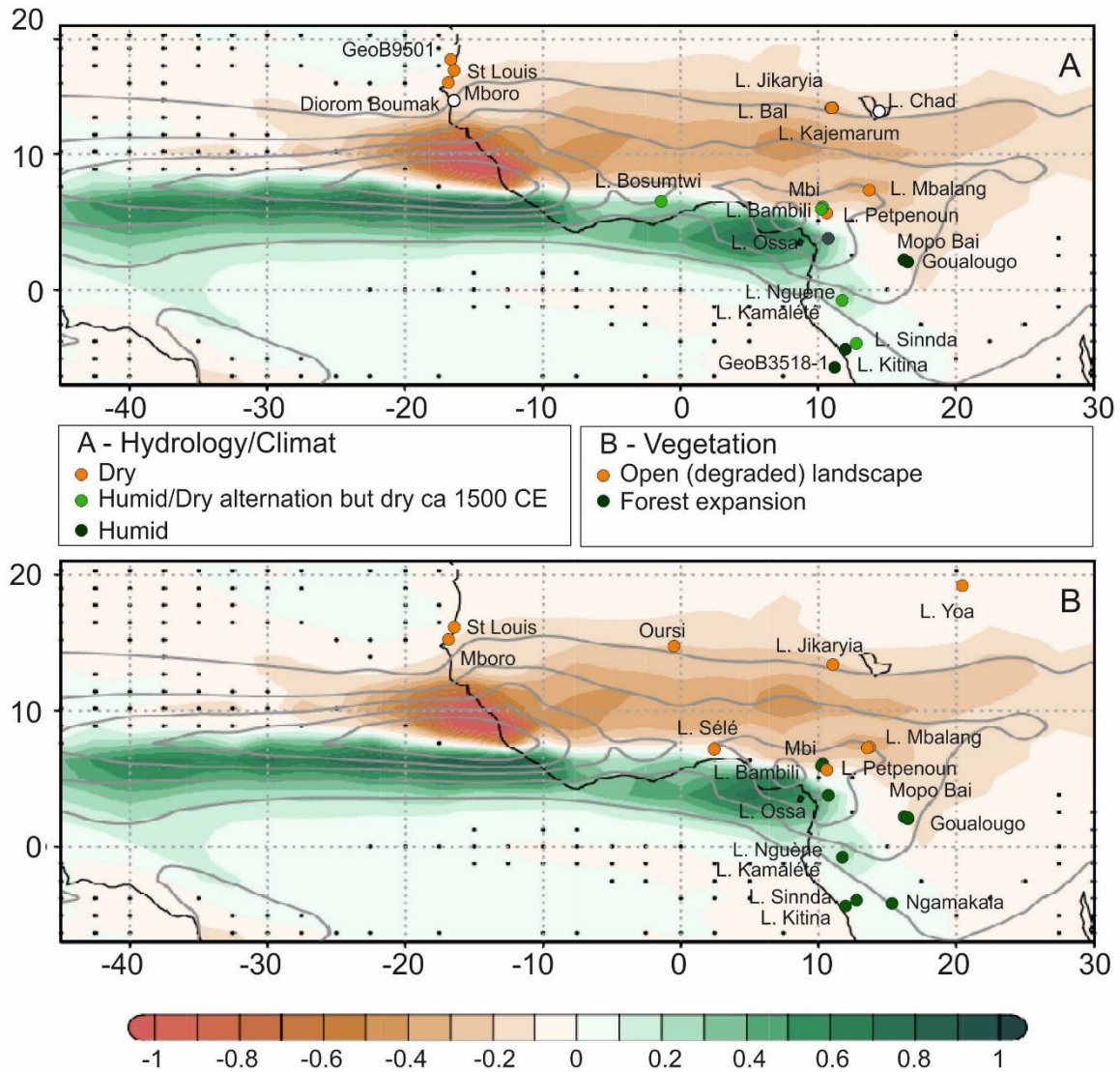
331 4. Discussion

332

333 4.1 Hydrology and Climate changes at secular timescale

334

335 Data and past1000 model simulations show a strong North-South contrast between the Sahel
 336 and Savannah zones, both subjected to severe drying during the LIA, and the equatorial areas,
 337 spanning the Gulf of Guinea coast, suggesting an overall change of the WAM.



338
339

340 **Figure 6:** Distribution of JAS rainfall anomalies difference between the LIA (1450-1849 CE) and
 341 the MCA (950-1249 CE) as simulated by the IPSL-CM6A-LR model in the past1000 ensemble-
 342 mean (shading, mm day^{-1}) compared to hydrological/dust (A) and vegetation (B) paleorecords
 343 during the LIA shown as dots following the same color scale as simulated anomalies. Grey
 344 contours indicate the piControl climatology from 2 mm day^{-1} in intervals of 4 mm day^{-1} .
 345 Stippling indicates disagreement across the three past1000 members on the sign of the
 346 represented difference.

347

348 The difference between the simulated past1000 JAS precipitation during the LIA and the MCA
 349 shows a characteristic distribution of a weakened WAM associated with a southward shift of
 350 the ITCZ, with less rainfall across the Sahel and more in the Gulf of Guinea coast (Fig. 6). These
 351 simulated anomalies are consistent with the overall distribution of hydrological and
 352 vegetation proxy reconstructions.

353

354 4.1.1 Hydrology

355

356 Three major regions can be recognized from the paleohydrological records: The Sahel and
357 Savannah zones, with drying trend; the center of the Congo Basin, which exhibit an opposite
358 trend of increasing humidity; and the boundary between the dry and humid domains defined
359 by the equatorial sectors closest to the coast or in mountain, where an alternation of wet and
360 dry phases is recorded. Two paleo-records differ from this general picture: that of Lake Chad,
361 where a period of flooding is recorded ca 1600CE, and that of the Diorom Boumak, where the
362 LIA is entirely characterized by a wet period (Fig. 4). As evoked above, the multiple origins of
363 the data and the complex hydrological system of Lake Chad may have introduced a bias into
364 the hydrological record and may explain (at least partly) the difference with the other Sahelian
365 archives. It is also likely that the rivers that feed the lake, which originate from southern
366 regions (the Chari and Logone rivers and their tributaries), may have caused an influx of water
367 during the short humid phase recorded on the Cameroon highlands (Bambili and Mbi) ca
368 1600CE. The case of the Diorom Boumak site is more complex: the historical records
369 mentioned by Maley and Vernet (2013) or Carré et al. (2019), among others, indicate that the
370 Saloum sector was wetter than the rest of the Sahel during part of the 16th century, allowing
371 for the establishment of two harvests per year. This may have been due, according to Maley
372 and Vernet (2013), to the occurrence of two rainy seasons, one in the core of the WAM season
373 in summer and another (usually of lesser importance) referred as “Heug rains” linked to polair
374 air intrusions in winter (Le Borgne 1979).

375

376 **4.1.2 Vegetation**

377

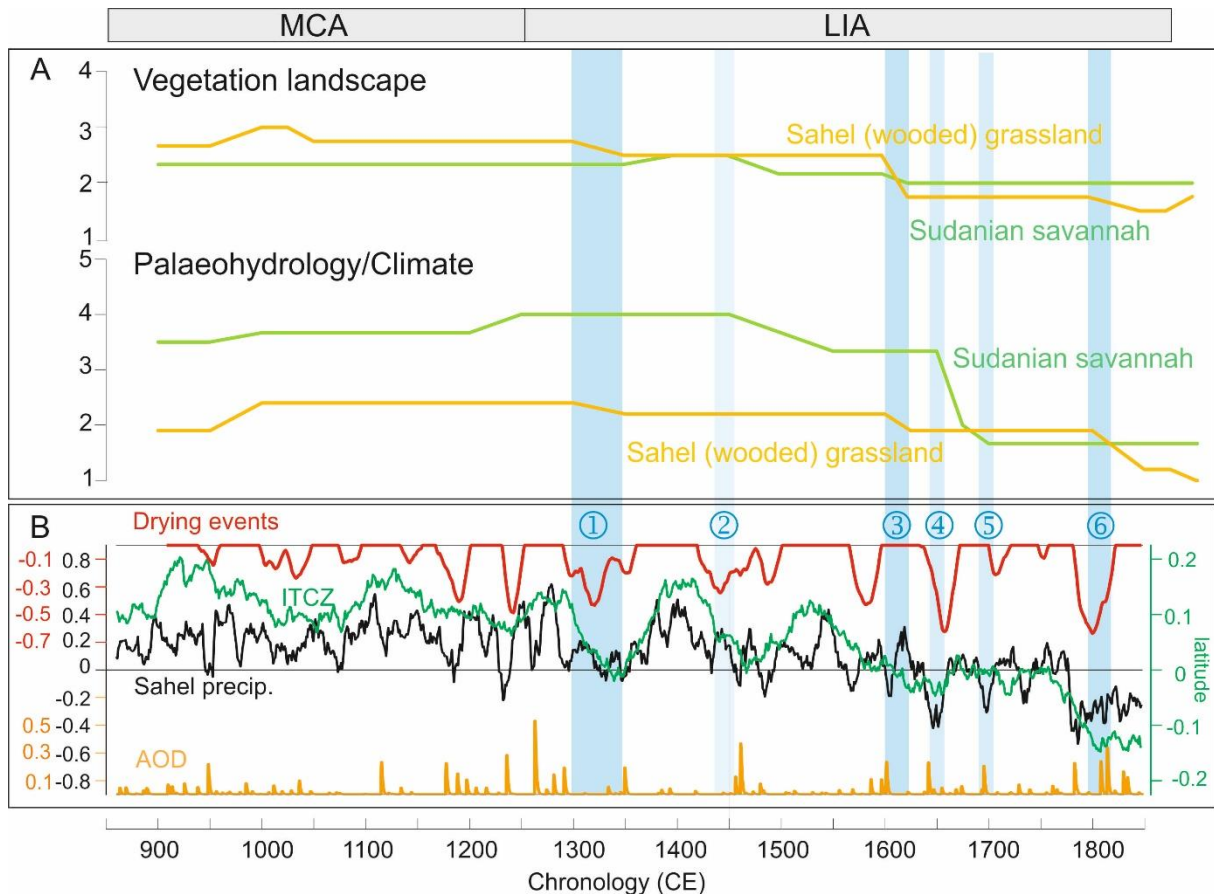
378 In the central Sahel, already degraded prior to the LIA (Lézine 2021), such as at Oursi, no
379 significant change occurred in the vegetation landscape which remained open throughout the
380 last millennium (Fig. 4B). The same pattern is observed in the wettest areas of the Congo Basin,
381 where the forests remained unchanged in composition and physiognomy (Tovar et al. 2019).
382 Elsewhere in the forest galleries of the Sahel and the Savannah zone (Mboro, St. Louis,
383 Petpenoun) the evolution of vegetation mirrored that of hydrological conditions while
384 recording a gradual degradation that culminated around 1800-1850 CE. In the westernmost
385 sector of the Sahel (Mboro, St Louis), the data suggest however a slight recovery of the
386 vegetation cover during the last few decades.

387 In contrast, both high and low elevation sites from the equatorial forest regions show an
388 opposite trend with marked forest recovery that began in the early years of the LIA and
389 accelerated around 1450CE. The forest expanded in the Equatorial lowlands despite increased
390 human presence has already been noted by Vincens et al. (1999). That means that the local
391 hydrological variations, and particularly the 1500 CE dry event, were of too small an amplitude
392 to impact forest dynamics. At most, a plateau in forest recovery is observed at that time
393 (Nguène, Kamalété). While the forest recovery was gradual at low altitudes, it seems to have
394 occurred more abruptly in the highlands.

395

396 **4.2 The chronology of events at multidecadal timescale: focus on the Sahel and Savannah** 397 **zone**

398



399
 400 **Figure 7:** Multiproxy records of hydrology and vegetation during the last millennium in the
 401 driest biomes (Sahel and Savannah zone) in western Africa (A) and long-term evolution of
 402 rainfall over the Sahel as simulated by the IPSL-CM6A-LR past1000 model (B). Panel B: (Black
 403 line) 10-year filtered ensemble-mean Sahel precipitation index (mm day^{-1}). (Green line) 50-
 404 year filtered anomalous latitudinal position of the JAS ITCZ (defined as the latitudinal
 405 maximum zonal-mean rainfall in $40^{\circ}\text{W}-10^{\circ}\text{E}$) in the past1000 simulations respectively to the
 406 piControl JAS mean position (in degrees of latitude). (Orange line) Global-mean AOD (volcanic
 407 forcing). (Red line) Sahel Drying Persistence Index defined as the 50-year running negative
 408 trend values over the Sahel ensemble-mean JAS precipitation index (mm day^{-1} per 50 years).
 409 Blue bars and numbers highlight the main climate/environmental degradation thresholds
 410 identified in the paleo-records.

411
 412 Environmental changes in the Sahel and Savannah zones during the LIA occurred in the context
 413 of widespread environmental degradation that followed the severe environmental crisis at
 414 the end of the African Humid Period (AHP; deMenocal et al., 2000). Between 3300 and 2500
 415 cal yr BP (Lézine, 2021), the forests and woodlands, that widely expanded across the plains
 416 and mountains of West Africa, strongly declined. This is particularly striking along the Atlantic
 417 coast of Senegal, between 15° and 17° N where specific environmental conditions related to
 418 the proximity of the sea and the presence of a water table near the surface favored the
 419 development of exceptionally dense forest galleries of humid tropical affinity during the AHP
 420 (Lézine 1989). As a result of this major environmental crisis, the Sahel and Savannah zone took
 421 on its modern aspect of semi-desert grassland and wooded grassland. In this context,
 422 discernible environmental fluctuations, particularly in vegetation, are of limited magnitude,
 423 with the exception of sectors where forest galleries were widely established during the AHP.

424

425 To discuss the chronology of events that punctuated the LIA, paleo-data were averaged in
 426 each geographical area (Sahel, Savannah zone) in the two categories covered by our study:
 427 hydrology/climate and vegetation (Fig. 7A). A Drying Persistence Index was constructed from
 428 our model results in order to quantify the Sahel precipitation deficit over at least 50-year
 429 periods (red curve in Fig. 7B). It is defined at each year as the negative linear trend of the Sahel
 430 ensemble-mean JAS precipitation (black curve in Fig. 7B) across the 50 previous years. We use
 431 50 years to be consistent with the multi-decadal to centennial temporal resolution of the
 432 paleo-data.

433 The past1000 simulations represent several drying events of various amplitude and duration
 434 during the MCA that do not correspond to any major change in the vegetation of the Sahel
 435 and Savannah zone. Instead, the environment in these two areas appears to be characterized
 436 by a relatively stable humid regime (Fig. 7A). This is coherent with the rainy mean state
 437 represented by the past1000 simulations over the MCA, which is associated with an
 438 anomalous northward ITCZ position (green curve in Fig. 7B) all over this period compared to
 439 the LIA.

440 At the end of the MCA, two early warning signals (Lenton 2011) of Sahel drying events centred
 441 at 1170 and 1240 CE are identified in our model experiments. The intensity and brevity of
 442 these two events contrast with the minor dry phases identified prior to the LIA since the onset
 443 of the last millennium. The Drying Persistence Index at these two events, which timing
 444 coincides with the occurrence of large clusters of volcanic eruptions (orange curve Fig. 7B),
 445 reaches over -0.3 mm day^{-1} across 50 years. Both events preceded the onset of the LIA gradual
 446 drying trend starting at 1250CE. This drying trend was sustained by the southward migration
 447 of the ITCZ which shifts south of the piControl mean position at 1600 CE. It is consistent with
 448 the continuous degradation of hydrological and vegetation conditions since 1250 CE in the
 449 Sahel and Savannah zone identified in our multi-proxy records.

450 Several abrupt drying events larger than those identified during the MCA punctuated the LIA,
 451 some of which reaching over -0.5 mm day^{-1} across 50 years. Despite the difference in temporal
 452 scale between the two approaches used here, there is a striking agreement between the major
 453 simulated droughts and the environmental degradation steps in our paleorecords (blue bars
 454 in Fig. 7). These degradation periods, in turn, span the largest eruptions from ca. 1250 to ca.
 455 1850CE, which are associated with the multi-decadal variability of Sahel precipitation over the
 456 past millennium in PMIP4 multi-model experiments.

457 **4.2.1 Steps in the degradation of the climate and the environment in the Sahel**

458 Three major steps are identified:

- 459 - The first dramatic environmental degradation occurred between 1290 and 1350 CE
 460 (event 1), i.e., ca. 50 years after the first warning signal and lasted about 60 years. Dust
 461 fluxes to the ocean, which had stabilized during the medieval warm period, increased
 462 (Mulitza et al. 2010) whereas lake levels dropped in the interdunal depressions in the
 463 western Sahel leading to the salinization of the waters (Lézine et al. 2019).
- 464 - The second stage in the degradation of environmental conditions occurred ca 1600CE
 465 (event 3). The environmental degradation was common to the entire Sahel (Bal,

466 Mboro, St Louis) while corresponding to a major collapse of the forest galleries at
 467 Mboro. Here also, a time lag of ca. 50 years can be observed between the onset of a
 468 drought phase and the response of the vegetation.

469 - The ultimate environmental threshold is recorded ca 1800CE (event 6). It resulted in
 470 the widespread lowering of lake levels, the massive contribution of dust to the ocean,
 471 and the irreversible destruction of forest galleries in the western Sahel in response to
 472 an abrupt drop in rainfall ca 1800CE, already observed by Carré et al. (2019) in the
 473 Saloum river delta. By accounting for a catastrophic decrease in precipitation of -0.6
 474 mm day⁻¹ over 50 years in our model experiments, this climatic tipping point related
 475 to closely spaced large volcanic eruptions (starting with Laki eruption in 1783 CE
 476 followed by the eruptions cluster over the 1809-1835 CE period including the 1815
 477 Tambora event), at the origin of the modern environmental conditions in the Sahel,
 478 was twice as large as the early warning signals identified at the end of the MCA.

479 Our data-model comparison suggests that there was a time lag of several decades (typically
 480 50 years) between the climate signal and the environmental response. If this time lag is highly
 481 probable, its duration and origin require further investigation. It may indeed result from the
 482 resilience of plants to climate change but we cannot exclude the memory effect of aquifers
 483 already observed by Aguiar et al. (2010) that may induce a delay between the climate signal
 484 and its effects on ecosystems. The uncertainty associated with the ages, whether it comes
 485 from the data or from the modelling, can also play a role by increasing or reducing this
 486 response time.

487

488 **4.2.2 The Savannah zone:**

489

490 As the ITCZ moved to more southerly latitudes, some of the drought events reconstructed in
 491 the Sahel had a major impact in the Savannah zone. Here, data is particularly sparse and, as in
 492 the Sahel, changes in vegetation are hardly distinguishable in these already highly degraded
 493 environments, such as at Lake Sélé (Salzmann et al. 2005). It is at Lake Petpenoun (Catrain
 494 2021) that the evidence is the clearest due to the presence of a gallery forest and pronounced
 495 hydrological changes at the core site.

496 We find that the last step of degradation of the savannah vegetation occurred during event 3
 497 also observed in the Sahel. Events 2 (1447-1493CE), 4 (1643-1657CE) and 5 (1691-1707CE)
 498 correspond only to phases of hydrological degradation that are not reflected in the regional
 499 vegetation. Data are still too rare to generalize this observation to the entire Savannah zone
 500 and could only account for local conditions.

501

502 **5. Conclusion**

503

504 Despite the uncertainties associated with data scarcity and heterogeneity, our study shows a
 505 remarkable agreement between the data and our past1000 model experiments for
 506 reconstructing the climate and environmental changes in response to natural forcing that
 507 characterized the LIA in western Africa. It highlights a North-South contrast between the
 508 dryness of the Sahel and the humidity of the equatorial zone. Despite the major difficulty
 509 related to the type of vegetation at play in the Sahel and the Savannah zone already degraded
 510 since the end of the AHP, major steps in the degradation of the environment can be identified.
 511 Our most remarkable results consists in (1) the identification of two early warning signals at

512 1170 and 1240CE, i.e. prior to the progressive LIA drying of the Sahel that lead to the climatic
513 tipping point at 1800-1850CE. This tipping point marks the setting of arid conditions (the driest
514 condition since 850CE) which still persist today; (2) the identification of abrupt drought events
515 which punctuated the LIA, the most important of them has impacted both the Sahel and the
516 Savannah zone ca. 1600CE. The consistency between proxy records and our model
517 experiments suggests a strong role of large volcanic eruptions in shaping Sahel environmental
518 changes over the pre-industrial millennium. Further work relying on large ensembles of
519 climate and vegetation models will help assess such hypothesis.

520

521 **Code availability**

522

523 The IPSL-CM6A-LR model code used in this work was frozen (version 6.1.0) and subsequently
524 altered only for correcting diagnostics or allowing further options and configurations. Versions
525 6.1.0 to 6.1.11 are therefore bit-reproducible for a given domain decomposition, compiling
526 options and supercomputer. LMDZ, XIOS, NEMO and ORCHIDEE are released under the terms
527 of the CeCILL licence. OASIS-MCT is released under the terms of the Lesser GNU General Public
528 License (LGPL). IPSL-CM6A-LR code (version 6.1.0) is publicly available through Apache
529 Subversion (svn) control system, with the following command lines under Linux: `svn co`
530 `http://forge.ipsl.jussieu.fr/igcmg/svn/modipsl/trunk modipsl; cd modipsl/util; ./model`
531 `IPSLCM6.1.11-LR` (IPSL-CM model development team, 2021). The `mod.def` file provides
532 information regarding the different revisions used, namely (1) NEMOGCM branch
533 `nemov36STABLE` revision 9455; (2) XIOS2 branches/`xios-2.5` revision 1873; (3) IOIPSL/src svn
534 tags/`v224`; (4) LMDZ6 branches/`IPSLCM6.0.15` rev 3643; (5) tags/`ORCHIDEE20/ORCHIDEE`
535 revision 6592; (6) OASIS3-MCT 2.0branch (rev 4775 IPSL server). The login and password
536 combination requested at first use to download the ORCHIDEE component is “anonymous”
537 and “anonymous”. We recommend referring to the project website,
538 http://forge.ipsl.jussieu.fr/igcmg_doc/wiki/Doc/Config/IPSLCM6 (IGCMG, 2022), for a proper
539 installation and compilation of the environment (version 6.1.10).

540

541 **Data availability**

542

543 Pollen data are available on the African Pollen Database website:
544 <https://africanpollendatabase.ipsl.fr>. The other paleo-data are from the literature.

545

546 The IPSL-CM6A-LR model data and pre-processed model and proxies datasets used in this
547 study are available at: <https://doi.org/10.5281/zenodo.7003853>

548

549 **Author contribution**

550

551 AML and MK designed the study. MK performed the IPSL-CM6A-LR model past1000
552 simulations and JV the simulations analysis. MC and AML collected and analyzed the data.
553 AML prepared the manuscript with contributions from all co-authors.

554

555 **Competing interests**

556

557 The authors declare that they have no conflict of interest

558

559 **Acknowledgements**

560

561 This work contributes to the ACCEDE ANR Belmont Forum project (18 BELM 0001 05). This
 562 work was undertaken in the framework of the French L-IPSL LABEX and the IPSL Climate
 563 Graduate School EUR and benefited from the FNS "SYNERGIA EffeCts of lArge voLcanic
 564 eruptions on climate and societies: UnDerstanding impacts of past Events and related
 565 subsidence cRises to evaluate potential risks in the future" (CALDERA) project under French
 566 CNRS grant agreement number CRSII5_183571 – CALDERA. MK acknowledges support from
 567 the HPC resources of TGCC under the allocations 2020-A0080107732 and 2021-A0100107732
 568 (project gencmip6) provided by GENCI (Grand Equipement National de Calcul Intensif) and
 569 2020225424 provided by PRACE (Partnership for Advanced Computing in Europe). This study
 570 benefited from the ESPRI computing and data centre (<https://mesocentre.ipsl.fr>) which is
 571 supported by CNRS, Sorbonne Université, Ecole Polytechnique and CNES as well as through
 572 national and international grants. Thanks are due to the African Pollen Database for data
 573 access. AML, MC and JV were funded by CNRS, and MK by IRD. We acknowledge the World
 574 Climate Research Programme's Working Group on Coupled Modelling.

575

576 **References**

- 577 Aguiar, L., Garneau, M., Lézine, A.-M., Maugis, P.: Evolution de la nappe des sables
 578 quaternaires dans la région des Niayes du Sénégal (1958-1994) : relation avec le climat
 579 et les impacts anthropiques. *Sécheresse* 21, 1-8, 10.1684/sec.2010.0237, 2010.
- 580 Aumont, O., Éthé, C., Tagliabue, A., Bopp, L., and Gehlen, M.: PISCES-v2. An ocean
 581 biogeochemical model for carbon and ecosystem studies. *Geosci. Model Develop.*, 8(8),
 582 2465-2513, 10.5194/gmd-8-2465-2015, 2015.
- 583 Ballouche, A.: Dynamique des paysages végétaux sahélo-soudaniens et pratiques agro-
 584 pastorales à l'Holocène : exemples au Burkina Faso. *Bull. Asso. Géogr. Français*, 75(2),
 585 191-200, 1998.
- 586 Bertaux, J., Sifeddine, A., Schwartz, D., Vincens, A., and Elenga, H.: Enregistrement
 587 sédimentologique de la phase sèche d'Afrique Equatoriale c. 3000 BP par la
 588 spectrométrie IR dans les lacs Sinnda et Kitina (Sud Congo). In « Dynamique à long terme
 589 des écosystèmes forestiers intertropicaux », Paris, ORSTOM, pp. 213-215, 1998.
- 590 Boucher, O., Servonnat, J., Albright, A.L., Aumont, O., Balkanski, Y., Bastrikov, V., Bekki, S.,
 591 Bonnet, R., Bony, S., Bopp, L. et al.: Presentation and evaluation of the IPSL-CM6A-LR
 592 climate model. *J. Adv. Model Earth Syst.*, 12(7), e2019MS002010,
 593 10.1029/2019MS002010, 2020.
- 594 Brncic, T.M., Willis, K.J., Harris, D.J., and Washington, R.: Culture or climate? The relative
 595 influences of past processes on the composition of the lowland Congo rainforest.
 596 *Philosoph. Trans. Royal Soc. B., Biol. Sci.*, 362(1478), 229-242, 10.1098/rstb.2006.1982,
 597 2007.
- 598 Brncic, T.M., Willis, K.J., Harris, D.J., Telfer, M.W., and Bailey, R. M.: Fire and climate change
 599 impacts on lowland forest composition in northern Congo during the last 2580 years
 600 from palaeoecological analyses of a seasonally flooded swamp. *Holocene*, 19, 79–89,
 601 10.1177/0959683608098954, 2009.
- 602 Carré, M., Azzoug, M., Zaharias, P., Camara, A., Cheddadi, R., Chevalier, M., Fiorillo, D., Gaye,
 603 A.T., Janicot, S., Khodri, M., Lazar, A., Lazareth, C.E., Mignot, J., Mitma Garcia, N., Patris,
 604 N., Perrot, O., and Wade, M.: Modern drought conditions in western Sahel

- 605 unprecedented in the past 1600 years. *Climate Dynamics*, 52(3), 1949-1964,
606 10.1007/s00382-018-4311-3, 2019.
- 607 Catrain, M.: *Le Petit Age de Glace en Afrique équatoriale : apport de l'étude palynologique des*
608 *sédiments du lac de Petpenoun, Cameroun. Unpublished Ms Thesis. University of Paris*
609 *Saclay, 2021.*
- 610 Coquery-Vidrovitch, C.: *Écologie et histoire en Afrique noire. Histoire, économie et société,*
611 483-504, 1997.
- 612 Descroix, L., Diogue Niang, A., Panthou, G., Bosdian, A., Sane, Y., Dacosta, H., Malam Abdou,
613 M., Vandervaere, J.P., and Quantin, G.: *Evolution récente de la pluviométrie en Afrique*
614 *de l'Ouest à travers deux regions: la Sénégalie et le bassin du Niger moyen.*
615 *Climatologie* 12, 25-43, 2015.
- 616 d'Orgeval, T., Polcher, J., and de Rosnay, P.: *Sensitivity of the West African hydrological cycle*
617 *in ORCHIDEE to infiltration processes. Hydro. Earth Syst. Sci.,* 12(6), 1387-1401,
618 10.5194/hess-12-1387-2008, 2008.
- 619 Demenocal, P., Ortiz, J., Guilderson, T., Adkins, J., Sarnthein, M., Baker, L., and Yarusinsky, M.:
620 *Abrupt onset and termination of the African Humid Period: rapid climate responses to*
621 *gradual insolation forcing. Quatern. Sci. Rev.,* 19(1-5), 347-361, 10.1016/S0277-
622 3791(99)00081-5, 2000.
- 623 Deser C., Alexander, M.A., Xie, S.P., et al.: *Sea surface temperature variability: Patterns and*
624 *mechanisms. Annual review of Marine Science* 2, 115–143. 10.1146/annurev-marine-
625 120408-151453, 2010.
- 626 Elenga, H.: *Végétation et climat du Congo depuis 24 000 ans B. P: analyse palynologique de*
627 *séquences sédimentaires du Pays Bateke et du littoral. PhD, Aix-Marseille III, 1992.*
- 628 Elenga, H., Schwartz, D., Vincens, A., Bertaux, J., de Namur, C., Martin, L., Wirrmann, D., and
629 Servant, M.: *Diagramme pollinique holocène du lac Kitina (Congo): mise en évidence de*
630 *changements paléobotaniques et paléoclimatiques dans le massif forestier du*
631 *Mayombe. C. R. Acad. Sci., Série 2a,* 323, 403-410, 1996.
- 632 Fofana, C.A.K., Sow, E., and Lézine, A.-M.: *The Senegal River during the last millennium. Rev.*
633 *Palaeobot. Palynol.* 275, 104175, 10.1016/j.revpalbo.2020.104175, 2020.
- 634 Folland, C.K., Palmer, T.N., and Parker, D.E.: *Sahel rainfall and worldwide sea temperatures,*
635 1901–85. *Nature*, 320, 602–607, 10.1038/320602a0, 1986.
- 636 Gadgil, S.: *The monsoon system: Land–sea breeze or the ITCZ? J. Earth Syst. Sci.* 127, 1.
637 10.1007/s12040-017-0916-x, 2018.
- 638 Gallego, D., Ordóñez, P., Ribera, P., Peña-Ortiz, C., and García-Herrera, R.: *An instrumental*
639 *index of the West African Monsoon back to the nineteenth century. Quarter. J. Royal*
640 *Meteo. Soc.,* 141(693), 3166-3176, 10.1002/qj.2601, 2015.
- 641 Giannini, A., Saravanan, R., and Chang, P.: *Oceanic forcing of Sahel rainfall on interannual to*
642 *interdecadal time scales. Science,* 302, 1027–1030, 10.1126/science.1089357, 2003.
- 643 Holmes, J.A., Allen, M.J., Street-Perrott, F.A., Ivanovich, M., Perrott, R.A., and Waller, M.P.:
644 *Late Holocene palaeolimnology of Bal Lake, northern Nigeria, a multidisciplinary study.*
645 *Palaeogeogr., Palaeoclimatol., Palaeoecol.,* 148(1-3), 169-185, 10.1016/S0031-
646 0182(98)00182-5, 1999.
- 647 Hourdin, F., Rio, C., Grandpeix, J.Y., Madeleine, J.B., Cheruy, F., Rochetin, N., Jam, A., Musat,
648 I., Idelkadi, A., Fairhead, L., Foujols, M.A., Mellul, L., Traore, A.K., Dufresne, J.L., Boucher,
649 O., Lefebvre, M.P., Millour, E., Vignon, E., Jouhaud, J., Diallo, F.B., Lott, F., Gastineau, G.,
650 Caubel, A., Meurdesoif, Y., and Ghattas, J.: *LMDZ6A: the atmospheric component of the*

- 651 IPSL climate model with improved and better tuned physics. *J. Adv. Model. Earth Syst.*
 652 12(7): e2019MS001892, 10.1029/2019MS001892, 2020.
- 653 Jungclauss, J. H., Bard, E., Baroni, M., Braconnot, P., Cao, J., Chini, L. P., Egorova, T., Evans, M.,
 654 Gonzalez-Rouco, J.F., Goose, H., Hurtt, G.C., Joos, F., Kaplan, J.O., Khodri, M., Goldewijk,
 655 K.K., Krivova, N., LeGrance, A.N., Lorenz, S.J., Luterbacher, J., Man, W., Maucock, A.C.,
 656 Mainshausen, M., Moberg, A., Muscheler, R., Nehbass-Ahles, C., Otto-Bliesner, B.I.,
 657 Phipps, S.J., Pongratz, J., Rozanov, E., Schmidt, G.A., Schmidet, H., Schmutz, W., Schurer,
 658 A., Shapiro, A.I., Sigl, M., Smerdon, J.E., Solanki, S.K., Timmreck, C., Toohey, M., Usoskin,
 659 ILGL, Wagner, S., Wu, C.J., Yeo, K.L., Zanchettin, D., Zhang, Q., and Zorita, E. : The PMIP4
 660 contribution to CMIP6–Part 3: The last millennium, scientific objective, and
 661 experimental design for the PMIP4 past1000 simulations. *Geosci. Model Dev.*, 10(11),
 662 4005-4033. 10.5194/gmd-10-4005-017, 2017.
- 663 Kageyama, M., Albani, S., Braconnot, P., Harrison, S. P., Hopcroft, P. O., Ivanovic, R. F.,
 664 Lambert, F., Marti, O., Peltier, W.R., Peterschmitt, J.Y., Roche, D.M., Tarasov, L., Zhang,
 665 X., Brady, E.C., Haywood, A.M., LeGrande, A.N., Lunt, D.J., Mahowald, N.M.,
 666 Mikolajewicz, U., Nisancioglu, K.H., Otto-Bliesner, B.L., Renssen, H., Tomas, R.A., Zhang,
 667 Q., Abe-Ouchi, A., Bartlein, P.J., Cao, J., Li, Q., Lohmann, G., Ohgaito, R., Shi, X., Volodin,
 668 E., Yoshida, K., Zhang, X., and Zheng, W. : The PMIP4 contribution to CMIP6–Part 4:
 669 Scientific objectives and experimental design of the PMIP4-CMIP6 Last Glacial Maximum
 670 experiments and PMIP4 sensitivity experiments. *Geosci. Model Dev.*, 10(11), 4035-4055,
 671 10.5194/gmd-10-4035-2017, 2017.
- 672 Kanamitsu, M., Ebisuzaki, W., Woollen, J., Yang, S.-K., Hnilo, J.J., Fiorino, M., and Potter, G.L.:
 673 NCEP-DOE AMIP-II Reanalysis (R-2), *Bull. Amer. Meteor. Soc.*, 83, 1631-1643,
 674 0.1175/BAMS-83-11-1631, 2002
- 675 Kucharski, F., Molteni, F., King, M.P., Farneti, R., Kang, I.S., and Feudale, L.: On the need of
 676 intermediate complexity general circulation models : A “SPEEDY” example. *Bull. Amer.*
 677 *Meteo. Soc.*, 94(1), 25-30, 10.1175/BAMS-D-11-00238.1, 2013.
- 678 Lawrence, D. M., Hurtt, G. C., Arneeth, A., Brovkin, V., Calvin, K. V., Jones, A. D., Jones, C. D.,
 679 Lawrence, P. J., de Noblet-Ducoudré, N., Pongratz, J., Seneviratne, S. I., and Shevliakova,
 680 E.: The Land Use Model Intercomparison Project (LUMIP) contribution to CMIP6:
 681 rationale and experimental design, *Geosci. Model Dev.*, 9, 2973–2998,
 682 <https://doi.org/10.5194/gmd-9-2973-2016>, 2016.
- 683 Le Borgne, J.: Un exemple d'invasion polaire sur la région mauritano-sénégalaise. *Annales*
 684 *Géogr.*, 489, 521-548, 1979.
- 685 Lebamba, J., Vincens, A., Lézine, A.-M., Marchant, R., and Buchet, G.: Forest-savannah
 686 dynamics on the Adamawa plateau (Central Cameroon) during the “African humid
 687 period” termination : A new high-resolution pollen record from Lake Tizong. *Rev.*
 688 *Palaeobot. Palynol.*, 235, 129-139, 10.1016/j.revpalbo.2016.10.001, 2016.
- 689 Lenton, T.M.: Early warning of climate tipping points. *Nature Climate Change* 1, 201-209,
 690 10.1038/nclimate1143, 2011.
- 691 Lézine, A.M., Lemonnier, K., and Fofana, C.A.K.: Sahel environmental variability during the last
 692 millennium: insight from a pollen, charcoal and algae record from the Niayes area,
 693 Senegal. *Rev. Palaeobot. Palynol.* 271, 104103, 10.1016/j.revpalbo.2019.104103, 2019.
- 694 Lézine, A.M.: Late Quaternary vegetation and climate of the Sahel. *Quatern. Res.*, 32, 317-334,
 695 10.1016/0033-5894(89)90098-7, 1989.
- 696 Lézine, A.M., Holl A., Lebamba J., Vincens A., Assi-Khadjis C., Février L., and Sultan
 697 E.: Temporal relationship between Holocene human occupation and vegetation change

- 698 along the northwestern margin of the Central African rainforest. *C. R. Géosci.*, 345, 327-
699 335, 10.1016/j.crte.2013.03.001, 2013.
- 700 Lézine, A.M., Lemonnier, K., Waller, M.P., Bouimetarhan, I., Dupont, L. and APD contributors :
701 Changes in the West African Landscape at the end of the African Humid Period.
702 *Palaeoecology of Africa* 35, 65-83, 10.1201/9781003162766-6, 2021
- 703 Lézine, A.M., Zheng, W., Braconnot, P., Krinner, G.: Late Holocene plant and climate evolution
704 at Lake Yoa, northern Chad: pollen data and climate simulations. *Clim. Past* 7, 1351-
705 1362, 10.5194/cp-7-1351-2011, 2011.
- 706 Maley, J., and Vernet, R. : *Peuples et évolution climatique en Afrique nord-tropicale, de la fin*
707 *du Néolithique à l'aube de l'époque moderne. Afriques. Débats, Méthodes et Terrains*
708 *d'Histoire*, 04, 10.4000/afriques.1209, 2013.
- 709 Matthes, K., Funke, B., Andersson, M. E., Barnard, L., Beer, J., Charbonneau, P., Clilverd, M. A.,
710 Dudok de Wit, T., Haberleiter, M., Hendry, A., Jackman, C. H., Kretzschmar, M.,
711 Kruschke, T., Kunze, M., Langematz, U., Marsh, D. R., Maycock, A. C., Misios, S., Rodger,
712 C. J., Scaife, A. A., Seppälä, A., Shanguan, M., Sinnhuber, M., Tourpali, K., Usoskin, I.,
713 van de Kamp, M., Verronen, P. T., and Versick, S.: Solar forcing for CMIP6 (v3.2), *Geosci.*
714 *Model Dev.*, 10, 2247–2302, <https://doi.org/10.5194/gmd-10-2247-2017>, 2017.
- 715 McPhaden, M.J., Zebiak, S.E., and Glanz, M.H.: ENSO as an integrating concept in earth
716 science. *Science*, 314, 5806, 1740-1745, 10.1126/science.1132588, 2006.
- 717 Meinshausen, M., Vogel, E., Nauels, A., Lorbacher, K., Meinshausen, N., Etheridge, D. M.,
718 Fraser, P. J., Montzka, S. A., Rayner, P. J., Trudinger, C. M., Krummel, P. B., Beyerle, U.,
719 Canadell, J. G., Daniel, J. S., Enting, I. G., Law, R. M., Lunder, C. R., O'Doherty, S., Prinn,
720 R. G., Reimann, S., Rubino, M., Velders, G. J. M., Vollmer, M. K., Wang, R. H. J., and Weiss,
721 R.: Historical greenhouse gas concentrations for climate modelling (CMIP6), *Geosci.*
722 *Model Dev.*, 10, 2057–2116, <https://doi.org/10.5194/gmd-10-2057-2017>, 2017.
- 723 Mohino, E., Janicot, S., and Bader, J.: Sahel rainfall and decadal to multi-decadal sea surface
724 temperature variability. *Clim. Dyn.*, 37(3), 419-440, 10.1007/s00382-010-0867-2, 2011.
- 725 Mulitza, S., Heslop, D., Pittauerova, D., Fischer, H. W., Meyer, I., Stuut, J. B., Zabel, M.,
726 Mollenhauer, G., Collins, J.A., Kuhnert, H., and Schulz, M.: Increase in African dust flux
727 at the onset of commercial agriculture in the Sahel region. *Nature*, 466(7303), 226-228,
728 10.1038/nature09213, 2010.
- 729 Nash, D.J., De Cort, G., Chase, B.M., Verschuren, D., Nicholson, S.E., Shanahan, T.M., Asrat,
730 A., Lézine, A.M., and Grab, S.W.: African hydroclimatic variability during the last 2000
731 years. *Quatern. Sci. Rev.*, 154, 1-22, 10.1016/j.quascirev.2016.10.012, 2016.
- 732 Ngomanda, A., Jolly, D., Bentaleb, I., Chepstow-Lusty, A., M'voubou Makaya, Maley, J.,
733 Fontune, M., Oslisly, R., Rabenkogo, N.: Lowland forest response to hydrological changes
734 during the last 1500 years in Gabon, Western Equatorial Africa. *Quatern. Res.* 60, 411-
735 425, 10.1016/j.yqres.2008.12.002, 2007.
- 736 Nguetsop, V. F., Bentaleb, I., Favier, C., Martin, C., Bietrix, S., Giresse, P., Servant-Vildary, M.,
737 and Servant, M.: Past environmental and climatic changes during the last 7200 cal yr BP
738 in Adamawa plateau (Northern-Cameroun) based on fossil diatoms and sedimentary
739 carbon isotopic records from Lake Mbalang. *Clim. Past*, 7(4), 1371-1393, 10.5194/cp-7-
740 1371-2011, 2011.
- 741 Nguetsop, V.F., Bentaleb, I., Favier, C., Bietrix, S., Martin, C., Servant-Vildary, S., and Servant,
742 M.: A late Holocene palaeoenvironmental record from Lake Tizong, northern Cameroon
743 using diatom and carbon stable isotope analyses. *Quatern. Sci. Rev.*, 72, 49-62,
744 10.1016/j.quascirev.2013.04.005, 2013.

- 745 Nguetsop, V.F., Servant-Vildary, S., Servant, M., and Roux, M.: Long and short-time scale
746 climatic variability in the last 5500 years in Africa according to modern and fossil diatoms
747 from Lake Ossa (Western Cameroon). *Global Planet. Change*, 72(4), 356-367,
748 10.1016/j.gloplacha.2010.01.011, 2010.
- 749 Nicholson, S.E.: The West African Sahel: A review of recent studies on the rainfall regime and
750 its interannual variability. *Intern. Scholar. Res. Not.*, 453521, 10.1155/2013/453521,
751 2013.
- 752 Nicholson, S.E.: Climatic variations in the Sahel and other African regions during the past five
753 centuries. *J. Arid Env.*, 1(1), 3-24, 10.1016/S0140-1963(18)31750-6, 1978.
- 754 Nicholson, S.E.: The nature of rainfall fluctuations in subtropical West Africa. *Monthly Weather*
755 *Rev.*, 108(4), 473-487, 10.1175/1520-0493(1980)108<0473:TNORFI>2.0.CO;2, 1980.
- 756 Nicholson, S.E.: The West African Sahel: A review of recent studies on the rainfall regime and
757 its interannual variability. *Intern. Scholar. Res. Notices*, 2013, 453521,
758 10.1155/2013/453521, 2013.
- 759 Nicholson, S.E., Klotter, D., and Dezfuli, A.K.: Spatial reconstruction of semi-quantitative
760 precipitation fields over Africa during the nineteenth century from documentary
761 evidence and gauge data. *Quat. Res.*, 78, 13–23, 10.1016/j.yqres.2012.03.012, 2012
- 762 Pham-Duc, B., Sylvestre, F., Papa, F., Frappart, F., Bouchez, C. and Crétaux, J.F.: The Lake Chad
763 hydrology under current climate change. *Nature scientific Reports* 10, 5498, /s41598-
764 020-62417-w, 2020.
- 765 Reynaud-Farrera, I., Maley, J., and Wirrmann, D.: Végétation et climat dans les forêts du Sud-
766 Ouest Cameroun depuis 4770 ans BP : analyse pollinique des sédiments du Lac Ossa. *CR*
767 *Acad. Sci. Paris*, 322(série II a), 749-755, 1996.
- 768 Rodríguez-Fonseca, B., Mohino, E., Mechoso, C. R., Caminade, C., Biasutti, M., Gaetani, M.,
769 Garcia-Serrano J., Vízny E. K., Cook K., Xue Y. K., Polo I., Losada T., Druyan L., Fontaine B.,
770 Bader J., Doblas-Reyes F. J., Goddard L., Janicot Serge, Arribas A., Lau W., Colman A.,
771 Vellinga M., Rowell D. P., Kucharski F., and Voltaire, A. : Variability and predictability of
772 West African droughts: a review on the role of sea surface temperature anomalies. *J.*
773 *Clim.*, 28(10), 4034-4060, 10.1175/JCLI-D-14-00130.1., 2015.
- 774 Rousset, C., Vancoppenolle, M., Madec, G., Fichefet, T., Flavoni, S., Barthélemy, A., Benshila,
775 R., Chanut, J., Lévy, C., Masson, S., and Vivier, F.: The louvain-la-neuve sea ice model
776 LIM3.6: global and regional capabilities. *Geosci. Model. Dev.* 8(10), 2991–3005,
777 10.5194/gmd-8-2991-2015, 2015.
- 778 Salzmann, U., and Hoelzmann, P.: The Dahomey Gap: an abrupt climatically induced rain forest
779 fragmentation in West Africa during the late Holocene. *Holocene*, 15(2), 190-199,
780 10.1191/0959683605hl799rp, 2005.
- 781 Schefuß, E., Schouten, S., and Schneider, R.R.: Climatic controls on central African hydrology
782 during the past 20,000 years. *Nature*, 437(7061), 1003-1006, 10.1038/nature03945,
783 2005.
- 784 Shanahan, T.M., Overpeck, J.T., Anchukaitis, K.J., Beck, J.W., Cole, J.E., Dettman, D.L., Peck,
785 J.A., Scholz, A., and King, J.W.: Atlantic forcing of persistent drought in West Africa.
786 *Science*, 324(5925), 377-380, 10.1126/science.1166352, 2009.
- 787 Street-Perrott, F.A., Holmes, J.A., Waller, M.P., Allen, M.J., Barber, N.G.H., Fothergill, P. A.,
788 Harkness, D.D., Ivanovich, M., Kroon, D. and Perrott, R.A.: Drought and dust deposition
789 in the West African Sahel: a 5500-year record from Kajemarum Oasis, northeastern
790 Nigeria. *Holocene*, 10(3), 293-302, 10.1191/095968300678141274, 2000.

- 791 Tovar, C., Harris, D.J., Breman, E., Brncic, T., and Willis, K.J.: Tropical monodominant forest
792 resilience to climate change in Central Africa: A *Gilbertiodendron dewevrei* forest pollen
793 record over the past 2,700 years. *J. Veget. Sci.*, 30(3), 575-586, 10.1111/jvs.12746, 2019.
- 794 Toohey, M., and Sigl, M.: Volcanic stratospheric sulfur injections and aerosol optical depth
795 from 500 BCE to 1900 CE, *Earth Syst. Sci. Data*, 9, 809–831, 10.5194/essd-9-809-2017,
796 2017.
- 797 Villamayor, J., Mohino, E., Khodri, M., Mignot, J., and Janicot, S.: Atlantic control of the late
798 nineteenth-century Sahel humid period. *J. Clim.*, 31(20), 8225-8240, 10.1175/JCLI-D-18-
799 0148.1, 2018.
- 800 Vincens, A., Buchet, G., Elenga, H., Fournier, M., Martin, L., de Namur, C., Schwartz, D., Servant,
801 M., and Wirrmann, D.: Changement majeur de la végétation du lac Sinnda (vallée du
802 Niari, Sud Congo) consécutif à l'assèchement climatique holocène supérieur : apport de
803 la palynologie. *C.R. Acad. Sci. Paris*, 318, 1521-1526, 1994.
- 804 Vincens, A., Schwartz, D., Bertaux, J., Elenga, H., and de Namur, C.: Late Holocene climatic
805 changes in western equatorial Africa inferred from pollen from Lake Sinnda, southern
806 Congo. *Quatern. Res.* 50(1), 34-45, 10.1006/qres.1998.1979, 1998.
- 807 Vincens, A., Schwartz, D., Elenga, H., Reynaud-Farrera, I., Alexandre, A., Bertaux, J., Mariotti,
808 A., Martin, L., Meunier, J.D., Nguetsop, F., Servant, M., Servant-Vildary, S., and
809 Wirrmann, D.: Forest response to climate changes in Atlantic Equatorial Africa during
810 the last 4000 years BP and inheritance on the modern landscapes. *J. Biogeogr.*, 26(4),
811 879-885, 10.1046/j.1365-2699.1999.00333.x, 1999.
- 812 Waller, M.P., Street-Perrott, F.A., and Wang, H.: Holocene vegetation history of the Sahel:
813 pollen, sedimentological and geochemical data from Jikariya Lake, north-eastern
814 Nigeria. *J. Biogeogr.*, 34(9), 1575-1590, 10.1111/j.1365-2699.2007.01721.x, 2007.
- 815 Wang, H., Holmes, J.A., Street-Perrott, F.A., Waller, M.P., and Perrott, R. A. Holocene
816 environmental change in the West African Sahel: sedimentological and mineral-
817 magnetic analyses of lake sediments from Jikariya Lake, northeastern Nigeria. *J.*
818 *Quatern. Sci.*, 23(5), 449-460, 10.1002/jqs.1154, 2008.
- 819
820